HHS Public Access

Author manuscript

J Cell Physiol. Author manuscript; available in PMC 2020 August 01.

Published in final edited form as:

J Cell Physiol. 2019 August ; 234(8): 12745–12756. doi:10.1002/jcp.27894.

Detection of Extracellular Vesicles in the Mouse Vaginal Fluid: Their Delivery of Sperm Proteins that stimulate Capacitation and modulate Fertility

Zeinab Fereshteh[1,2], **Pradeepthi Bathala**[1], **Deni S. Galileo**[1], and **Patricia A. Martin-DeLeon**[1]

[1]Department of Biological Sciences, University of Delaware, Newark, DE 19716

[2]Department of Biomedical Engineering, University of Delaware, Newark, DE, 19716

Abstract

Extracellular vesicles (EVs) were isolated by ultracentrifugation of vaginal luminal fluid (VLF) from superovulated mice, and identified for the first time using transmission electron microscopy. Characterized by size and biochemical markers (CD9 and HSC70), EVs were shown to be both microvesicular and exosomal and were dubbed as “Vaginosomes” (VGS). Vaginal cross-sections were analyzed to visualize EVs *in situ*: EVs were present in the lumen and also embedded between squamous epithelial and keratinized cells, consistent with their endogenous origin. Western blots detected PMCA1 and tyrosine-phosphorylated proteins in the VGS cargo and also in uterosomes. Flow cytometry revealed that following co-incubation of caudal sperm and VLF for 30 min, the frequencies of cells with the highest SPAM1, PMCA1/4, and PMCA1 levels increased 16.4-, 8.2- and 27-fold, respectively; compared to control co-incubated in PBS. Under identical conditions sperm tyrosine-phosphorylated proteins were elevated ~3.3-fold, after VLF co-incubation. Progesterone-induced acrosome reaction (AR) rates were significantly ($P<0.001$) elevated in sperm co-incubated with VGS for 10–30 min, compared to PBS. Sperm artificially deposited in the vaginas of superovulated females for these periods also showed significant ($P<0.01$) increases in AR rates, compared to PBS. Thus *in vitro* and *in vivo*, sperm acquire from the vaginal environment factors that induce capacitation, explaining recent findings for their acrosomal status in the isthmus. Overall, VGS appear to deliver higher levels of proteins involved in preventing premature capacitation and AR than those promoting them. Our findings which have implications for humans open the possibility of new approaches to infertility treatment with exosome therapeutics.

Keywords

vaginal exosomes; sperm capacitation; Ca^{2+} efflux pumps; acrosome reaction uterosomes; tyrosine-phosphorylated proteins

Corresponding author: 219 McKinly Lab, Univ. Delaware, Newark, DE 19716, Tel: 302- 831-2249: Fax: 302-831-2281, pdeleon@udel.edu.

Introduction

Extracellular vesicles (EVs) are spherical membranous organelles released by epithelial cells into body fluids where they play a role in cell-to-cell communication by conveying molecules from one cell or tissue to another (Thery et al., 2002; Valadi et al., 2007). These nano-sized organelles carry a variety of regulatory molecules such as proteins, microRNAs, RNAs and lipids (Thery et al., 2002; Valadi et al., 2007), and have been identified in both male and female reproductive biofluids (Martin-DeLeon, 2016). In the male, EVs in the epididymal luminal fluid (ELF), dubbed epididymosomes, and those in the seminal plasma, prostasomes, have been extensively studied (Saez and Sullivan, 2016; Sullivan, 2016). It has been well-established that epididymosomes are responsible for the transfer of a variety proteins to sperm to facilitate epididymal maturation and the re-modeling of the sperm membrane (Caballero et al., 2010; Sullivan and Saez, 2013). On the other hand, prostasomes have been known to transfer proteins that regulate sperm function, such as motility, and those that have a stimulatory effect on capacitation, as well as those with an inhibitory effect on this process (Arienti et al., 1998a; Siciliano et al., 2008).

Compared to the well-characterized EVs in male secretions, EVs in the female reproductive fluids have received very little attention as the studies have only just been emerging. In the female tract EVs have been identified in the uterine luminal fluid (ULF) of mice (Griffiths et al., 2008a; Griffiths et al., 2008b), sheep (Burns et al., 2014), and humans (Ng et al., 2013) where they have been dubbed uterosomes; and in the oviductal luminal fluid (OLF) in mice (Al-Dossary et al., 2013), bovine (Alminana et al., 2017; Lopera-Vasquez et al., 2016), and humans (Bathala et al., 2018), where they are referred to as oviductosomes. During the murine estrus, uterosomes and oviductosomes were shown to carry both glycosyl phosphatidylinositol- (GPI-) linked and transmembrane proteins that can be transferred to sperm *in vitro* (Al-Dossary et al., 2013; Griffiths et al., 2008b). Notable among the GPI-linked proteins that uterosomes carry and deliver to sperm, is the highly conserved Sperm adhesion molecule 1 (SPAM1) which is known to play multiple roles in sperm function (Martin-DeLeon, 2011). Importantly, it was shown that following uterosomal transfer of SPAM1 to murine sperm during their co-incubation with ULF, there was increased hyaluronic acid binding capacity and cumulus penetration efficiency of sperm (Griffiths et al., 2008b).

An essential transmembrane protein that is present in the uterine and oviductal epithelia and in the cargoes of uterosomes and oviductosomes is Plasma membrane Ca^{2+}- ATPase 4 (PMCA4) (Al-Dossary et al., 2013). It is the major calcium efflux pump in murine sperm (Wennemuth et al., 2003), and its absence results in male infertility (Okunade et al., 2004). Interestingly, in the mouse PMCA4 is most highly expressed in estrus where it is not only present in the ULF and the OLF via uterosomes and oviductosomes, but is also found in the vaginal luminal epithelium and the vaginal luminal fluid (VLF) (Al-Dossary et al., 2013). However, in the vaginal epithelium and VLF it exists in significantly lower abundance than in the uterine and oviductal counterparts (Al-Dossary et al., 2013). This is in contrast to SPAM1 which was not studied in the VLF, but was detected in the vaginal luminal epithelium (which releases proteins into the luminal fluid) in significantly greater abundance than in oviductal tissues (Zhang and Martin-DeLeon, 2003). Thus, the abundance of a

protein that is released in the luminal fluids appears to be dependent on the particular protein rather than the region of the reproductive tract from which it is released during estrus. Following co-incubation of murine sperm with the combined luminal fluids (OLF, ULF, and VLF), PMCA4 could be delivered to sperm *in vitro* (Al-Dossary et al., 2013), suggesting that this occurs *in vivo*.

Oviductosomes have been shown to transfer PMCA4 to murine sperm, using super-resolution structured illumination microscopy (SR-SIM), by a fusogenic mechanism (Al-Dossary et al., 2015). This mechanism which was also reported for protein transfer to sperm from bovine epididymosomes (Schwarz et al., 2013) appears to be conserved, since uterosome-like vesicles secreted by human endometrial epithelial cells *in vitro* were shown to fuse with sperm following a 15-min co-incubation period (Franchi et al., 2016). This fusion of the uterosome-like vesicles stimulated capacitation by significantly increasing sperm protein tyrosine-phosphorylation, a hallmark of capacitation (Baker et al., 2006; Kwon et al., 2014; Visconti et al., 1995).

Because membrane fusion that mediates the transfer of cargo constituents from EVs to sperm occurs in as short a time period as 15 min (Franchi et al., 2016), we were prompted to investigate the presence of EVs in the murine VLF during estrus and their ability to transfer proteins to sperm. Herein we show the presence of exosomes and microvesicles in murine VLF, and their ability to transfer fertility-modulating proteins in their cargo to sperm, following their co-incubation for 30 min. Importantly, we show the physiological consequence of protein transfer from vaginal EVs (vaginosomes, VGS) to sperm *in vitro* and *in vivo*, with respect to a significant increase in the rate of acrosome reaction after co-incubation for 10 min.

Material and Methods

Mice and Reagents

Sexually mature 10–12 week-old males and 4–12 week-old female mice (FVB/N and C57BL/6J strains; Harlan, Indianapolis, IN) were used for this study. In addition to these WT mice, *Pmca4*$^{-/-}$ males and females on the FVB/N background were used to obtain testis and vaginal tissues, luminal fluid, and EVs for Western blotting analysis. These mutant mice, generated in the laboratory of Dr. Gary Shull (University of Cincinnati), were a generous gift. They were bred and genotyped as described previously (Okunade et al., 2004). The studies were approved by the Institutional Animal Care and Use Committee at the University of Delaware and were in agreement with the Guide for the Care and Use of Laboratory Animals published by the National Research Council of the National Academies, 8th ed., Washington, D.C. (publication 85–23, revised 2011). All enzymes and chemicals were purchased from Fisher Scientific Co. (Malvern, PA), Sigma (St Louis, MO) or Invitrogen (Carlsbad, CA), unless otherwise specified.

Antibodies

Rabbit monoclonal anti-PMCA1 antibody (ab190355) and the isotype control (ab172730) were purchased from Abcam (Cambridge, MA) and used for Western blots, and flow

cytometric studies. Mouse monoclonal anti-HSC70 antibody (sc-7298), mouse monoclonal anti-panPMCA1/4 antibody (sc-20028), goat polyclonal pan-PMCA4 antibody (Y20, sc-22080), rat monoclonal anti-CD9 antibody (sc-18869), and anti-phosphotyrosine antibody (PY99) which is a mouse monoclonal (sc-7020) were purchased from Santa Cruz Biotechnology (Dallas, TX). Also mouse monoclonal anti-phosphotyrosine antibody (clone 4G10) was purchased from Millipore (Temecula, CA). A rabbit anti-mouse SPAM1 antiserum, a polyclonal antipeptide ([C]NEKGNASRRKESSD in the C-terminus [#381–395] custom-made by Zymed (South San Francisco, CA) and previously reported to be specific for SPAM1 via peptide inhibition (Deng et al., 2000; Zhang and Martin-DeLeon, 2003) was used. Secondary antibodies were purchased from Santa Cruz Biotech, Inc., Life Technologies or Molecular Probes Inc. (Eugene, OR). Fluoro-Gel II with DAPI (17985–50), used for immunofluorescence, was obtained from Electron microscope sciences (Hatfield, PA).

Staging of females and the Hormonal Induction of Estrus (Superovulation)

The stages of the estrus cycle of 8 to 12 week-old FVB/N virgins were classified based on the proportion of different cell types identified in the vaginal secretion (Byers et al., 2012). To hormonally induce estrus, 4 to 6 week-old FVB/N and C57BL/6J females were sequentially injected intraperitoneally with pregnant mare serum gonadotropin (PMSG, 7.5 i.u.) and human chorionic gonadotropin (HCG, 7.5 i.u.), 44–48 h apart. After 13.5–14 h from the last injection, females were sacrificed and their reproductive tissues collected for processing and analysis, as described below.

Collection of Vaginal Luminal Fluid and Isolation of Extracellular vesicles

Immediately after sacrificing females hormonally-induced into estrus, vaginas were removed. The luminal fluid was collected in PBS with protease inhibitors after mincing the vaginas as previously described for the oviduct (Al-Dossary et al., 2013). After mincing the tissues in PBS, the tissues were allowed to gravity settle and the fluid was clarified by centrifugation at 16,000 x g for 20 min to exclude cells, cells debris, and tissue fragments. The supernatant is referred to as the clarified vaginal luminal fluid (VLF), and was then frozen immediately at −80°C for further processing. Fresh or thawed frozen clarified VLF was subjected to ultracentrifugation at 120,000 x *g* at 4°C for 2 h using Beckman Optima 2–70 k ultracentrifuge and a Ti60 rotor, as described (Griffiths et al., 2008a). Resulting pellets (EVs) were re-suspended in homogenization buffer (62.5mM Tris-HCl, 10% glycerol, 1% SDS, pH 6.8) with protease inhibitor (1mM PMSF) for Western blot analysis, or in PBS for transmission electron microscopy (TEM) or further processing.

Negative staining for TEM

Aliquots of the VLF pellet suspension from females in estrus were negatively stained, using a methodology similar to that previously described (Al-Dossary et al., 2013; Griffiths et al., 2008a). Briefly, nickel TEM grids (Electron Microscopy Sciences, Hatfield, PA, USA), 400 mesh with formvar/carbon film were floated on a drop of the pellet suspension. Several drops of water were then used to wash the grids which were then stained with 1% uranyl acetate, a phospholipid stain, before being subjected to TEM (Zeiss LIBRA 120, Germany) analysis and image capture of the membrane vesicles.

Perfusion of mice for vaginal sectioning

The lumen of the vaginas of sexually mature FVB/N females were flushed with a glutaraldehyde /formaldehyde perfusate (2% each in PBS) immediately after sacrifice, and the vaginas fixed in 2% glutaraldehyde and 2% formaldehyde in 0.1M sodium cacodylate buffer pH 7.4 containing 2 mM calcium chloride. The tissue was cut into 1–2 mm^3 pieces. Samples were sectioned on a Reichert-Jung Ultracut E ultramicrotome, and sections collected onto 200 mesh formvar-carbon coated copper grids and post-stained with 2% uranyl acetate in 50% methanol and Reynolds lead citrate (Reynolds, 1963).

SDS-PAGE and Western blot analysis

Samples of homogenized EVs from VLF and of testicular tissues (used as positive control) for electrophoresis were diluted in 5X Laemelli sample buffer and heated at 95°C for 5 min. Twenty to 40 μg of proteins (or as specified) from tissues, fluids, or EVs were loaded in each lane of 10% polyacrylamide gels and transferred onto nitrocellulose membrane (Amersham Biosciences, UK). Blots were blocked for 1h at RT, incubated in anti-PMCA1 (1:2000) primary antibody or anti-CD-9 (1:1000), anti-phosphotyrosine (1:250), anti-PMCA1 overnight at 4°C, and processed as previously described (Al-Dossary et al., 2013). Membranes were re-probed with HSC70 antibody (1:1000), which served as an internal loading control for normalization and as an EV biomarker. The normalization approach was as described (http://bitesizebio.com/23411/the-4-important-steps-for-western-blot-quantification/). To quantify the intensity of the bands, images from shorter film exposures were selected and Image Lab 6 software (Bio-Rad) was used to subtract the background from the tyrosine-phosphorylated bands and that of the HSC70 (n = 3).

In Vitro Sperm Uptake of PMCA1, PMCA1/4, SPAM1, and tyrosine-phosphorylated proteins from VLF EVs

Aliquots of caudal sperm from C57BL/6J males were co-incubated with VLF EVs (total protein being 0.55 μg/μl) suspended in PBS or PBS (vehicle control) for 30 min or 3 h at 37°C and assayed for protein uptake by flow cytometry as previously described (Al-Dossary et al., 2013; Andrews et al., 2015). After co-incubation, sperm were washed with PBS and fixed in 1.5% paraformaldehyde for 1h at RT. After washing they were permeabilized with 0.1% triton X-100 for 10 min at RT. They were then washed with PBS and blocked with 2% BSA and treated with the primary antibodies diluted 1:200 for anti-PMCA1, 1:400 for SPAM1, and 1:50 for anti-phosphotyrosine, anti-PMCA1/4, and anti-PMCA4, followed by the appropriate secondary antibodies conjugated to Alexa Fluor 488 and subsequent washing. Uptake was quantified in 50,000 sperm, using the appropriate IgG control and a FACSCalibur (Becton Dickinson, San Diego, CA) flow cytometer equipped with an argon laser with excitation at 488 nm.

To examine immunolabeled sperm with confocal microscopy, aliquots of the sperm suspension used for flow cytometry were smeared on slides which were then counterstained with DAPI in Prolong Gold.

In Vivo Exposure of Caudal Sperm to the vaginal environment of superovulated females

C57BL/6J females were superovulated with hormonal injections as described above. Thirteen and one-half to 14 h after the last injection freshly collected caudal sperm were re-suspended in PBS and with the use of a pipette with an Eppendorf tip aliquots were deposited in the vagina of each female which was immobilized in a CO_2 chamber with a flow rate of 4–5 liters/min. Females were immediately removed from the chamber after depositing sperm and, after 30 min, were sacrificed to retrieve sperm from the vagina. In other experiments, 36×10^5 sperm were deposited in the vagina for 10, 15, 20, or 30 min, before females were sacrificed for recovery of sperm from the vagina. Sperm were collected after mincing the vaginal tissue in PBS. The tissue in the suspension was allowed to gravity settle and the supernatant was spun at 500 x g to collect the sperm. The control sperm were kept in PBS at 37°C and processed with the sperm collected from the vaginas for the frequency of acrosome- reacted cells.

Hyaluronic acid-enhanced Progesterone-induced Acrosome Reactions

The acrosome reaction was induced under physiological conditions using a modification of the method previously described (Morales et al., 2004; Smith et al., 2014). Briefly, caudal sperm samples that had been incubated with PBS or VGS re-constituted in PBS, or that had been deposited in the vagina were collected by centrifugation and washed in PBS. In the absence of incubation in a capacitating medium, they were then treated with 100 μg ml^{-1} hyaluronic acid for 30 min followed by progesterone (3.18 μmol l^{-1} for 5 min). Sperm were then pelleted (500 x *g*, 15 min) and re-suspended in 4% paraformaldehyde and stored overnight at 4^oC. The sperm were then re-suspended in PBS to prepare a 1:5 dilution of the samples and ~200 μl of the suspension was dragged across a clean glass slide and allowed to air-dry. Slides were then stained with 0.44% Coomassie Brilliant Blue G-250 in 60% methanol-acetic acid for 15 min. Alternatively, the acrosomal matrix of sperm on slides was stained with fluorescein isothiocyanate (FITC)-conjugated peanut agglutinin (PNA) lectin (L7381), 10 μg/ml, for 30 min in the dark. Slides were then washed in PBS 3 times and counterstained in DAPI with Prolong Gold. They were then examined under the confocal microscope (blindly) to determine the presence/absence of the acrosomal cap (in the case of Coomassie blue staining) or the green fluorescence signal for the acrosomal matrix, in a minimum of 200 sperm/sample from replicates of the assay.

Statistical Analysis

Data were processed using Chi-squared (χ^2) analysis with Yates correction for contingency tables. The Students' *t*-test was used to compare means of band intensities for Western blot analysis and the means of the percentages of cells with the highest fluorescence intensities in the flow cytometric analysis.

Results

Ultracentrifugation of VLF followed by negative staining of the resulting pellets which were analyzed by TEM revealed the presence of EVs of varying sizes. In Fig. 1A, we show that EVs of both exosomal (<100 nm) and microvesicular (100 nm −1μm) sizes are present and have dubbed them as "vaginosomes" (VGS). To show that these EVs have an endogenous

vaginal origin and are not transported to the vaginal fluid from the uterine fluid, we investigated their presence *in situ* by examining vaginal sections after perfusion of the tissue. TEM analysis of the sections show that the majority of EVs are entrapped in the vaginal tissue between keratinized and squamous epithelial cells, while others are present in the lumen (Fig. 1B).

Western analysis was employed for biochemical characterization of the EVs. Using oviductosomes as a positive control, we show the presence of the 24 kDa CD9 tetraspanin band in the VLF EVs, VGS (Fig. 2A). A second biochemical marker, HSC70, was detected in VGS via Western blot analysis. Western blots also showed the presence of a calcium efflux pump, Plasma membrane Ca^{2+}- ATPase 1 (PMCA1), before the membrane was stripped and re-probed for HSC70 (Fig. 2B).

To determine if VGS can transfer PMCAs and other proteins in their cargo to sperm, co-incubation assays were performed. After washing and processing the sperm for immunofluorescence, VGS were shown to be capable of delivering SPAM1, PMCA1/4, and PMCA1, to sperm (Fig. 3A). On the basis of the frequencies of sperm with the highest fluorescence intensity, flow cytometric analysis revealed an increase of 16.4-fold for SPAM1, 8.2-fold for PMCA1/4, and 27-fold for PMCA1 when sperm were co-incubated with VGS for 30 min, compared to the PBS control (Fig. 3A–a', b', c'). A *t*-test for the mean number of sperm with the highest fluorescence intensities shows significant differences ($P<0.01$) between sperm co-incubated in VGS and PBS for the 3 proteins (Fig. 3B). When the immunofluorescence was visualized by confocal microscopy, uptake of SPAM1 appeared to have occurred mostly on the flagellum while for PMCA1/4 both the flagellum and the head were involved (Fig. 3C). When co-incubation was extended for 3 h, there was only an ~3-fold increase in the proportion of sperm with the highest levels of PMCA4 on sperm for VGS/VLF, compared to PBS (Supplementary S1).

Based on the finding that tyrosine-phosphorylated proteins are delivered to human sperm by uterosome-like EVs (Franchi et al., 2016) and to mouse sperm by oviductosomes (Bathala et al., 2018), we performed Western blot analysis to investigate their presence in VGS as well as uterosomes (UTS). Using OVS as a positive control, 6 tyrosine- phosphorylated proteins (including those with MWs of ~55, 95, 130, and ~180 kDa) seen in OVS are present in the cargoes of both VGS and UTS (Fig. 4A). Although the bands for these proteins in OVS tend to be more intense than in those in VGS and UTS, when they were normalized as a group with HSC70 there were no significant differences in the mean intensities between pairs of the 3 EVs ($P = 0.18$ for OVS and UTS; $P = 0.38$ for OVS and VGS). However when the intensities of the 95 kDa band which is associated with the acrosome reaction (Kwon et al., 2014) were compared independently among the 3 EVs, those for the OVS and the UTS were found to be significantly ($P<0.001$) higher than that in VGS (Fig. 4A–b). Importantly, VGS were able to transfer these proteins to caudal sperm. Flow cytometric analysis showed a 3.3-fold increase in the frequency of cells with the highest fluorescence intensity/protein level when sperm were co-incubated for 30 min in re-constituted VGS, compared to PBS (Fig. 4B–b). This difference in frequency is significant ($P<0.001$), as shown in Fig. 4B–c. Confocal microscopy showed that uptake of tyrosine-phosphorylated proteins occurred on both the sperm head and the flagellum (Fig. 4C).

Finally, to investigate the physiological consequence of uptake of tyrosine-phosphorylated proteins, among other fertility-modulating proteins, we assessed the level of acrosome reaction at 0 (control), 10, 20, and 30 min of co-incubation of caudal sperm and VGS. Table 1 shows that while at 0 min the rate of acrosome -reacted sperm (distinguished in Fig. 5A) for the PBS (control) and VGS re-constituted in PBS at 0 min (control) were similar (32 and 31%,), they were higher (83.9 to 95.3%) for the re-constituted VGS, with fold change differences being 3.3 (10 min), 3.0 (20 min), and 2.6-fold (30 min), compared to the PBS. The grand total of acrosome-reacted sperm co-incubated in PBS and VGS averaged 29.2 and 75.7% (2.8-fold increase), respectively. The fold-changes represent significant ($P<0.001$) increases of acrosome–reacted sperm at each of the time points and the overall group, compared to the control. When the frequencies of acrosome-reacted sperm were investigated following co-incubation of sperm at various concentrations of VGS (undiluted, diluted 2x, 5x, 10x, 20x) for 10 min, a dose-response relationship was detected. However, at 20x (the lowest concentration) and 10x, the rates of acrosome-reacted sperm were significantly ($P<0.05$; $P<0.01$) higher than that seen for sperm co-incubated in PBS (Fig. 5B).

Additionally, sperm were exposed to the vaginal environment *in vivo*. When various numbers of caudal sperm were artificially deposited in the vagina for 30 min and sperm retrieved after sacrifice of the females, exposure to the vaginal environment resulted in significant ($P<0.001$) increases in the frequency of acrosome-reacted sperm, compared to the unexposed control held at 37°C (Fig. 5C). Similarly, when the same number of sperm were exposed to the vaginal environment for 10, 15 20, or 30 min there was a significant ($P<0.001$) increase in the frequency of acrosome-reacted sperm for 10 min (60%), compared to the PBS control (28%) with the longer exposures having higher frequencies (Fig. 5D).

To confirm the rates of acrosome reaction seen in sperm exposed to VGS and the PBS control, as reflected in the staining of the acrosomal cap, we assayed the rate of sperm with an intact acrosomal matrix, as detected by fluorescently labeled PNA (peanut agglutinin) lectin which is a biochemical marker of the acrosomal matrix (Guyonnet et al., 2014). In Fig. 6 we show PNA-positive and –negative sperm. Of 212 sperm co-incubated in PBS 143 or 67% were PNA-positive and 33% PNA-negative. On the other hand, 96 of 229 or 42% were PNA-positive and 58% were PNA-negative for sperm co-incubated in VGS. Chi-squared (χ^2) analysis of a 2 × 2 contingency table, with Yates correction, showed the difference to be highly significant ($P<0.01$); and indicates that the rate of PNA-negative sperm, which are acrosome-reacted, is dependent on the presence of VGS during co-incubation.

Discussion

Our results show that, like other female biofluids (Al-Dossary et al., 2013; Griffiths et al., 2008b), the murine vaginal luminal fluid contains membrane-bound vesicles that are released from the epithelial lining of the vagina. The detection of VGS *in situ* in vaginal sections is consistent with their release from the tissue into the lumen. These EVs, similar in sizes to those detected in the uterus and oviducts (Al-Dossary et al., 2013; Griffiths et al., 2008a), carry the characteristic biochemical markers (CD9 and HSC70) as well as sperm regulatory proteins including the PMCAs and tyrosine-phosphorylated proteins. As vaginal

exosomes are conserved in humans where they were shown to inhibit an early step of the HIV-1 life cycle (Smith & Daniel, 2016), it is highly likely that the sperm regulatory proteins detected in the mouse exosomes are also conserved in humans.

During mating in the mouse, sperm are deposited in the vagina where vaginal plugs are formed, promoting transport of the sperm to the uterus (Suarez and Pacey, 2006). We show that *in vitro* exposure of caudal sperm to VGS in the VLF for 30 min, compared to PBS, resulted in significantly higher numbers of sperm with elevated levels of PMCA1 (27-fold), PMCA1/4 (8.2 -fold), SPAM1 (16.4 -fold), and tyrosine- phosphorylated proteins (3.3-fold). When caudal sperm and VGS/VLF were co-incubated for 3 h, there was only a 3-fold increase in PMCA4, compared to the PBS control. It is likely that this lower level of uptake at 3 h reflects a lower level of sperm viability which is required for uptake as fluorescence recovery after photobleaching (FRAP) experiments show that uptake occurs in live cells (Al-Dossary et al., 2015).

As the mechanism of EV cargo delivery to sperm has been shown to be fusogenic (Al-Dossary et al., 2015; Schwarz et al., 2013), sperm-VGS interaction would be expected to enrich the sperm membrane with cholesterol and lipids. This enrichment would decrease its fluidity and consequently result in the prevention of premature capacitation and premature acrosome reaction, as shown for human sperm and their interaction with prostasomes (Arienti et al., 1998a; Arienti et al., 1998b; Carlini et al., 1997; Pons-Rejraji et al., 2011).

The levels of protein uptake in sperm after co-incubation may be related to their physiological roles. After 30 min co-incubation, the large increases of the PMCAs (8.2 – and 27-folds) which are Ca^{2+}efflux pumps are consistent with their role in keeping intracellular Ca^{2+} levels low and thus preventing premature capacitation and premature AR. In fact PMCA4, the major Ca^{2+}efflux pump in murine sperm (Wennemuth et al., 2003), is likely to be stimulated by the decapacitation factor reported by Adeoya-Osiguwa & Fraser (1996). On the other hand, the 3.3-fold increase in tyrosine-phosphorylated proteins which are known to stimulate capacitation (Baker et al., 2006; Kwon et al., 2014; Visconti et al., 1995) is an order of magnitude lower than the increases seen for the PMCAs and SPAM1 (16.4-fold) after 30 min of co-incubation. While SPAM1 is a hyaluronidase that facilitates sperm penetration in the cumulus matrix and the perivitelline space (Martin-DeLeon, 2011), the lower increase of tyrosine- phosphorylated proteins is of physiological consequence in incrementally stimulating capacitation. Evidence for this comes from our finding that a 10-min period of co-incubation of sperm with VGS *in vitro*, or *in vivo* (following exposure to the vaginal environment) resulted in the induction of the acrosome reaction, a hallmark of capacitated sperm. Table 1 and Fig. 5D show that significantly ($P<0.001$; $P<0.01$) more sperm were acrosome-reacted after co-incubation of sperm with VGS, compared to PBS.

That significantly more sperm were acrosome-reacted after co-incubation with VGS, compared to PBS, is consistent with the presence in VGS of the 95 kDa phosphorylated protein that is associated with the AR (Kwon et al., 2014; Leyton and Saling, 1989), and the delivery of these proteins to sperm. It should be noted that the AR in this study was progesterone–induced. Progesterone has been shown to induce an increase in cytosolic calcium in sperm and their fusion with prostasomes which contain calcium enhances the

calcium increase (Arienti et al., 2001). As we have detected calcium in oviductosomes (unpublished observation), it is highly likely to be present in VGS which after fusion with sperm would enhance the intracellular calcium induced by progesterone to a level that would prime sperm for the acrosome reaction.

A significant increase in acrosome-reacted sperm was also detected when porcine sperm were co-incubated with EVs isolated from seminal plasma (Siciliano et al., 2008). Thus VGS appear to play similar roles to prostasomes, with respect to inhibiting premature capacitation and premature acrosome reaction as well as promoting them. Based on the significantly increased number of sperm with elevated levels of proteins delivered by VGS, it appears that VGS play a more predominant role in inhibiting these physiological states than in promoting them. It should also be noted that SPAM1 is present in murine prostasomes (Zhang et al., 2004) which are also likely to carry PMCA4 which is present in human prostasomes (Andrews et al., 2015). It is thus conceivable that the high levels of PMCAs and SPAM1 that are delivered to sperm by VGS/VLF are accommodated by caudal sperm, since they have not yet been exposed to the prostatic/seminal fluid. Thus in the *in vivo* situation, ejaculated sperm might be likely to acquire lower levels of these proteins from VGS, by virtue of their interaction with, and prior uptake from, prostasomes. It is also likely that *in vivo* the length of time of exposure to the vaginal environment might be shorter than that used in the study.

Our results show a dose–response relationship with respect to the frequency of acrosome-reacted sperm after co-incubation with various concentrations of VGS. It is possible that the physiological concentration of VGS to which sperm are exposed *in vivo* is less than we have used *in vitro* since all of the VGS collected might not have been naturally released in the lumen. Thus we investigated the effect of sperm exposure to various dilutions of the VGS/VLF and detected that even for the most dilute concentration (20x) there was a significant increase in the number of acrosome-reacted sperm. Further, *in vivo* exposure of sperm to the vaginal environment also showed a significant increase in AR rates. Thus the observation that tyrosine-phosphorylated proteins, which are increased in sperm during capacitation (Kwon et al., 2014), can be delivered to sperm by VGS may provide an explanation for the recent findings of the acrosomal status of mouse sperm during their migration in the oviduct (Perez-Cerezales et al., 2018). Within recent years, the widely held view that the fertilizing spermatozoon begins its acrosome reaction on the zona pellucida of the oocyte and that sperm that have undergone this reaction earlier have lost their fertilizing potential, has been challenged (Perez-Cerezales et al., 2018).

Inoue et al. (2011) have shown that mouse oocytes are fertilizable by sperm that completed the AR before entering the cumulus oophorus. They reported that sperm which acrosome-reacted long before contacting the zona pellucida maintained their ability to traverse it and to effect fertilization (Inoue et al., 2011). Further, Hino et al. (2016) have shown that mouse sperm acrosome-react during sperm migration in the lower and upper isthmus of the oviduct. Interestingly, it has been reported that almost all fertilizing mouse sperm within the oviduct begin to acrosome-react before their ascent to the ampulla from the isthmus, although nothing is known of the inducing factor(s) involved (Hino et al., 2016; Jin et al., 2011; La Spina et al., 2016; Muro et al., 2016). Our findings for the transfer of tyrosine-

phosphorylated proteins to sperm by VGS, and their presence in murine uterosomes and oviductosomes (Fig. 4A) as recently shown by Bathala et al. (2018), allow us to propose that murine sperm are primed to acrosome-react during their transit in the vagina, uterus, and oviduct by the acquisition of tyrosine-phosphorylated proteins from EVs present in the luminal fluids of all three organs. This conclusion is consistent with the reported delivery of tyrosine-phosphorylated proteins by uterosomal-like vesicles to human sperm (Franchi et al., 2016). Our data therefore provide an answer to a question that has puzzled investigators for some time, namely “What induces the acrosome reaction of mouse sperm within the isthmus” (Hino et al., 2016)?. Thus, the present findings fill an important gap in our knowledge of the induction of murine sperm capacitation and the resulting AR.

Our results also open the possibility of treating some types of infertility in which there is a deficiency of fertility-modulating sperm proteins. As EVs are currently being explored for clinical applications, the possibility exists that engineered EVs could be used to deliver missing proteins to sperm in patients who carry genetic mutations (Barkalina et al., 2015). As humans are like mice, with respect to sperm delivery in the vagina which is readily accessible, engineered EVs could be provided in the vaginal fluid or in the form of a suppository, to allow the delivery of relevant proteins to sperm.

Supplementary Material

Refer to Web version on PubMed Central for supplementary material.

Acknowledgements.

Thanks are extended to Shannon Modla and Chandran Sabanayagam of the Bioimaging Center at Delaware Biotechnology Institute for assistance with transmission electron microscopy and confocal microscopy, respectively.

The work was supported by NIH-5P20RR015588 and NIH-RO3HD073523.

References

Adeoya-Osiguwa SA, Fraser LR. 1996 Evidence for Ca(2+)-dependent ATPase activity, stimulated by decapacitation factor and calmodulin, in mouse sperm. Molecular Reproduction and Development 44: 111–120. [PubMed: 8722699]

Al-Dossary AA, Bathala P, Caplan JL, Martin-DeLeon PA. 2015 Oviductosome-Sperm Membrane Interaction in Cargo Delivery: Detection of fusion and underlying Molecular Players using 3D Super-Resolution Structured Illumination Microscopy (SR-SIM). The Journal of Biological Chemistry 290 :17710–17723. [PubMed: 26023236]

Al-Dossary AA, Strehler EE, Martin-DeLeon PA. 2013 Expression and secretion of plasma membrane Ca2+-ATPase 4a (PMCA4a) during murine estrus: association with oviductal exosomes and uptake in sperm. PloS One 8: e80181. [PubMed: 24244642]

Alminana C, Corbin E, Tsikis G, Alcantara-Neto AS, Labas V, Reynaud K, Galio L, Uzbekov R, Garanina AS, Druart X, Mermillod P. 2017 Oviduct extracellular vesicles protein content and their role during oviduct-embryo cross-talk. Reproduction 154 :153–168.

Andrews RE, Galileo DS, Martin-DeLeon PA. 2015 Plasma membrane Ca2+-ATPase 4: interaction with constitutive nitric oxide synthases in human sperm and prostasomes which carry Ca2+/CaM-dependent serine kinase. Molecular Human Reproduction 21 :832–843. [PubMed: 26345709]

Arienti G, Carlini E, De Cosmo AM, Di Profio P, Palmerini CA. 1998a Prostasome-Like Particles in Stallion Semen1. Biology of Reproduction 59: 309–313. [PubMed: 9687300]

Arienti G, Carlini E, Polci A, Cosmi EV, Palmerini CA. 1998b Fatty acid pattern of human prostasome lipid. Archives of Biochemistry and Biophysics 358: 391–395. [PubMed: 9784255]

Arienti G, Nicolucci A, Santi F, Carlini E, Palmerini CA. 2001 Progesterone-induced increase of sperm cytosolic calcium is enhanced by previous fusion of spermatozoa to prostasomes. Cell Calcium 30: 222–227. [PubMed: 11509001]

Baker MA, Hetherington L, Aitken RJ. 2006 Identification of SRC as a key PKA-stimulated tyrosine kinase involved in the capacitation-associated hyperactivation of murine spermatozoa. Journal of Cell Science 119: 3182–3192. [PubMed: 16835269]

Barkalina N, Jones C, Wood MJ, Coward K. 2015 Extracellular vesicle-mediated delivery of molecular compounds into gametes and embryos: learning from nature. Human Reproduction Update 21: 627–639. [PubMed: 26071427]

Bathala P, Fereshteh Z, Li K, Al-Dossary AA, Galileo DS, Martin-DeLeon PA. 2018 Oviductal extracellular vesicles (oviductosomes, OVS) are conserved in humans: murine OVS play a pivotal role in sperm capacitation and fertility. Molecular Human Reproduction 24 :143–157. [PubMed: 29370405]

Burns G, Brooks K, Wildung M, Navakanitworakul R, Christenson LK, Spencer TE. 2014 Extracellular vesicles in luminal fluid of the ovine uterus. PloS One 9: e90913. [PubMed: 24614226]

Byers SL, Wiles MV, Dunn SL, Taft RA. 2012 Mouse estrous cycle identification tool and images. PloS One 7: e35538. [PubMed: 22514749]

Caballero J, Frenette G, Sullivan R. 2010 Post testicular sperm maturational changes in the bull: important role of the epididymosomes and prostasomes. Veterinary Medicine International 2011:757194. [PubMed: 20981306]

Carlini E, Palmerini CA, Cosmi EV, Arienti G. 1997 Fusion of sperm with prostasomes: effects on membrane fluidity. Archives of Biochemistry and Biophysics 343: 6–12. [PubMed: 9210640]

Deng X, He Y, Martin-DeLeon PA. 2000 Mouse Spam1 (PH-20): Evidence for its Expression in the Epididymis and for a New Category of Spermatogenic-Expressed Genes. Journal of Andrology 21: 822–832.. [PubMed: 11105908]

Franchi A, Cubilla M, Guidobaldi HA, Bravo AA, Giojalas LC. 2016 Uterosome-like vesicles prompt human sperm fertilizing capability. Molecular Human Reproduction 22: 833–841. [PubMed: 27678485]

Griffiths GS, Galileo DS, Reese K, Martin-DeLeon PA. 2008a Investigating the role of murine epididymosomes and uterosomes in GPI-linked protein transfer to sperm using SPAM1 as a model. Molecular Reproduction and Development 75: 1627–1636. [PubMed: 18384048]

Griffiths GS, Miller KA, Galileo DS, Martin-DeLeon PA. 2008b Murine SPAM1 is secreted by the estrous uterus and oviduct in a form that can bind to sperm during capacitation: acquisition enhances hyaluronic acid-binding ability and cumulus dispersal efficiency. Reproduction 135: 293–301. [PubMed: 18299422]

Guyonnet B, Egge N, Cornwall GA. 2014 Functional amyloids in the mouse sperm acrosome Molecular and Cellular Biol 34: 2624–2634.

Hino T, Muro Y, Tamura-Nakano M, Okabe M, Tateno H, Yanagimachi R. 2016 The Behavior and Acrosomal Status of Mouse Spermatozoa In Vitro, and Within the Oviduct During Fertilization after Natural Mating. Biology of Reproduction 95: 50. [PubMed: 27417908]

Inoue N, Satouh Y, Ikawa M, Okabe M, Yanagimachi R. 2011 Acrosome-reacted mouse spermatozoa recovered from the perivitelline space can fertilize other eggs. Proceedings of the National Academy of Sciences of the United States of America 108: 20008–20011. [PubMed: 22084105]

Jin M, Fujiwara E, Kakiuchi Y, Okabe M, Satouh Y, Baba SA, Chiba K, Hirohashi N. 2011 Most fertilizing mouse spermatozoa begin their acrosome reaction before contact with the zona pellucida during in vitro fertilization. Proceedings of the National Academy of Sciences of the United States of America 108: 4892–4896. [PubMed: 21383182]

Kwon WS, Rahman MS, Pang MG. 2014 Diagnosis and prognosis of male infertility in mammal: the focusing of tyrosine phosphorylation and phosphotyrosine proteins. Journal of Proteome Research 13: 4505–4517. [PubMed: 25223855]

La Spina FA, Puga Molina LC, Romarowski A, Vitale AM, Falzone TL, Krapf D, Hirohashi N, Buffone MG. 2016 Mouse sperm begin to undergo acrosomal exocytosis in the upper isthmus of the oviduct. Developmental Biology 411: 172–182. [PubMed: 26872876]

Leyton L, Saling P. 1989 95 kd sperm proteins bind ZP3 and serve as tyrosine kinase substrates in response to zona binding. Cell 57: 1123–1130. [PubMed: 2472220]

Lopera-Vasquez R, Hamdi M, Fernandez-Fuertes B, Maillo V, Beltran-Brena P, Calle A, Redruello A, Lopez-Martin S, Gutierrez-Adan A, Yanez-Mo M, Ramirez MA, Rizos D. 2016 Extracellular Vesicles from BOEC in In Vitro Embryo Development and Quality. PloS One 11: e0148083. [PubMed: 26845570]

Martin-DeLeon PA. 2011 Germ-cell hyaluronidases: their roles in sperm function. International Journal of Andrology 34: e306–318. [PubMed: 21418239]

Martin-DeLeon PA. 2016 Extracellular vesicles in the reproductive tracts: Roles in Sperm maturation and function. In: Meyer A, editor. Exosomes: Biogenesis, Therapeutic Applications and Emerging Research: Nova Biomedical, Nova Science Publishers p79–100.

Morales CR, Badran H, El-Alfy M, Men H, Zhang H, Martin-DeLeon PA. 2004 Cytoplasmic localization during testicular biogenesis of the murine mRNA for Spam1 (PH-20), a protein involved in acrosomal exocytosis. Molecular Reproduction and Development 69: 475–482. [PubMed: 15457544]

Muro Y, Hasuwa H, Isotani A, Miyata H, Yamagata K, Ikawa M, Yanagimachi R, Okabe M. 2016 Behavior of Mouse Spermatozoa in the Female Reproductive Tract from Soon after Mating to the Beginning of Fertilization. Biology of Reproduction 94: 80. [PubMed: 26962112]

Ng YH, Rome S, Jalabert A, Forterre A, Singh H, Hincks CL, Salamonsen LA. 2013 Endometrial exosomes/microvesicles in the uterine microenvironment: a new paradigm for embryo-endometrial cross talk at implantation. PloS One 8: e58502. [PubMed: 23516492]

Okunade GW, Miller ML, Pyne GJ, Sutliff RL, O'Connor KT, Neumann JC, Andringa A, Miller DA, Prasad V, Doetschman T, Paul RJ, Shull GE. 2004 Targeted ablation of plasma membrane Ca2+-ATPase (PMCA) 1 and 4 indicates a major housekeeping function for PMCA1 and a critical role in hyperactivated sperm motility and male fertility for PMCA4. The Journal of Biological Chemistry 279: 33742–33750. [PubMed: 15178683]

Perez-Cerezales S, Ramos-Ibeas P, Acuna OS, Aviles M, Coy P, Rizos D, Gutierrez-Adan A. 2018 The oviduct: from sperm selection to the epigenetic landscape of the embryo. Biology of Reproduction 98: 262–276. [PubMed: 29228115]

Pons-Rejraji H, Artonne C, Sion B, Brugnon F, Canis M, Janny L, Grizard G. 2011 Prostasomes: inhibitors of capacitation and modulators of cellular signalling in human sperm. International Journal of Andrology 34: 568–580. [PubMed: 21029115]

Reynolds ES. 1963 The use of lead citrate at high pH as an electron-opaque stain in electron microscopy. Journal of Cell Biology 17:208–212. [PubMed: 13986422]

Saez F, Sullivan R. 2016 Prostasomes, post-testicular sperm maturation and fertility. Front Biosci (Landmark Ed) 21:1464–1473. [PubMed: 27100516]

Schwarz A, Wennemuth G, Post H, Brandenburger T, Aumuller G, Wilhelm B. 2013 Vesicular transfer of membrane components to bovine epididymal spermatozoa. Cell and Tissue Research 353: 549–561. [PubMed: 23715721]

Siciliano L, Marciano V, Carpino A. 2008 Prostasome-like vesicles stimulate acrosome reaction of pig spermatozoa. Reproductive Biology and Endocrinology : 6:5. [PubMed: 18234073]

Smith JA, Daniel R (2016) Human vaginal fluid contains exosomes that have an inhibitory effect on an early step of the HIV-1 life cycle. AIDS 30: 2611–2616. [PubMed: 27536982]

Smith MA, Michael R, Aravindan RG, Dash S, Shah IS, Galileo DS, Martin-DeLeon PA. 2014 Anatase Titanium Dioxide Nanoparticles in Mice: Evidence for Induced Structural and Functional Sperm Defects after Short-, but not Long-, term Exposure. Asian J. Androl 10 24 doi: 10.4103/1008-682x.143247.

Suarez SS, Pacey AA. 2006 Sperm transport in the female reproductive tract. Human Reproduction Update 12: 23–37. [PubMed: 16272225]

Sullivan R 2016 Epididymosomes: Role of extracellular microvesicles in sperm maturation. Frontiers in Bioscience 8:106–114.

Sullivan R, Saez F. 2013 Epididymosomes, prostasomes, and liposomes: their roles in mammalian male reproductive physiology. Reproduction 146 :R21–35. [PubMed: 23613619]

Thery C, Zitvogel L, Amigorena S. 2002 Exosomes: composition, biogenesis and function. Nature Reviews Immunology 2: 569–579.

Valadi H, Ekstrom K, Bossios A, Sjostrand M, Lee JJ, Lotvall JO. 2007 Exosome-mediated transfer of mRNAs and microRNAs is a novel mechanism of genetic exchange between cells. Nature Cell Biology 9 :654–659. [PubMed: 17486113]

Visconti PE, Bailey JL, Moore GD, Pan D, Olds-Clarke P, Kopf GS. 1995 Capacitation of mouse sperm II. Protein tyrosine phosphorylation and capacitation are regulated by a cAMP-dependent pathway. Development 121:1139– 1150. [PubMed: 7538069]

Wennemuth G, Babcock DF, Hille B. 2003 Calcium clearance mechanisms of mouse sperm. The Journal of General Physiology 122: 115–128. [PubMed: 12835474]

Zhang H, Martin-DeLeon PA. 2003 Mouse Spam1 (PH-20) is a multifunctional protein: evidence for its expression in the female reproductive tract. Biology of Reproduction 69: 446–454. [PubMed: 12672666]

Zhang H, Morales CR, Badran H, El-Alfy M, Martin-DeLeon PA. 2004 Spam1 (PH-20) expression in the extratesticular duct and accessory organs of the mouse: a possible role in sperm fluid reabsorption. Biology of Reproduction 71: 1101–1107. [PubMed: 15175239]

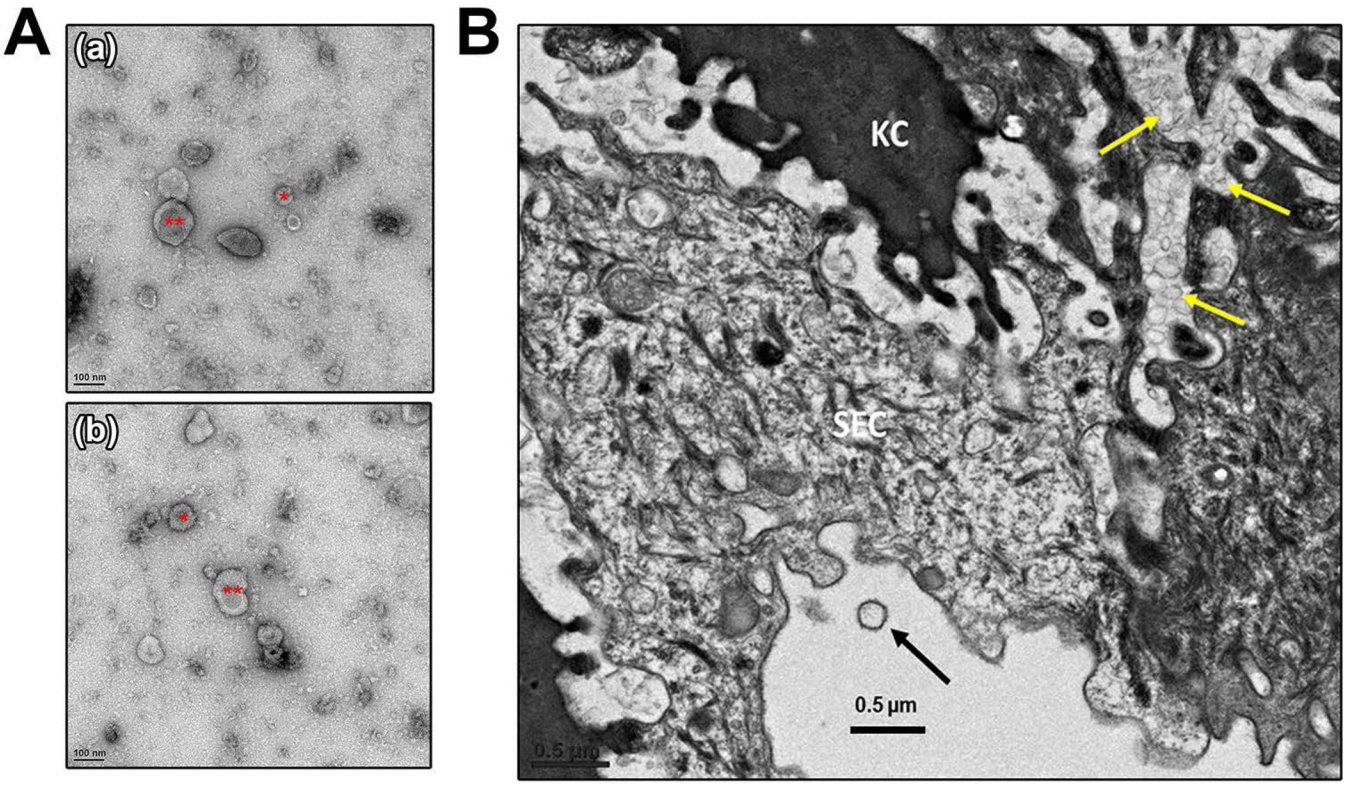

FIGURE 1:

Isolation of extracellular vesicles from vaginal luminal fluid (VLF) and their detection *in situ* in vaginal sections. A) Negative staining of TEM of the VLF pellet reveals the presence of extracellular vesicles of varying sizes, *exosomes of size < 100 nm and **microvesicles ranging in size from 100 nm to 1µm diameter. Both are referred to as vaginosomes (VGS). **B)** TEM image of a vaginal cross section showing the membrane vesicles that are present in between the layers of vaginal tissue, as indicated by yellow arrows. KC = Keratinized cells and SEC = Squamous epithelial cells. An EV is seen in the lumen (arrowed).

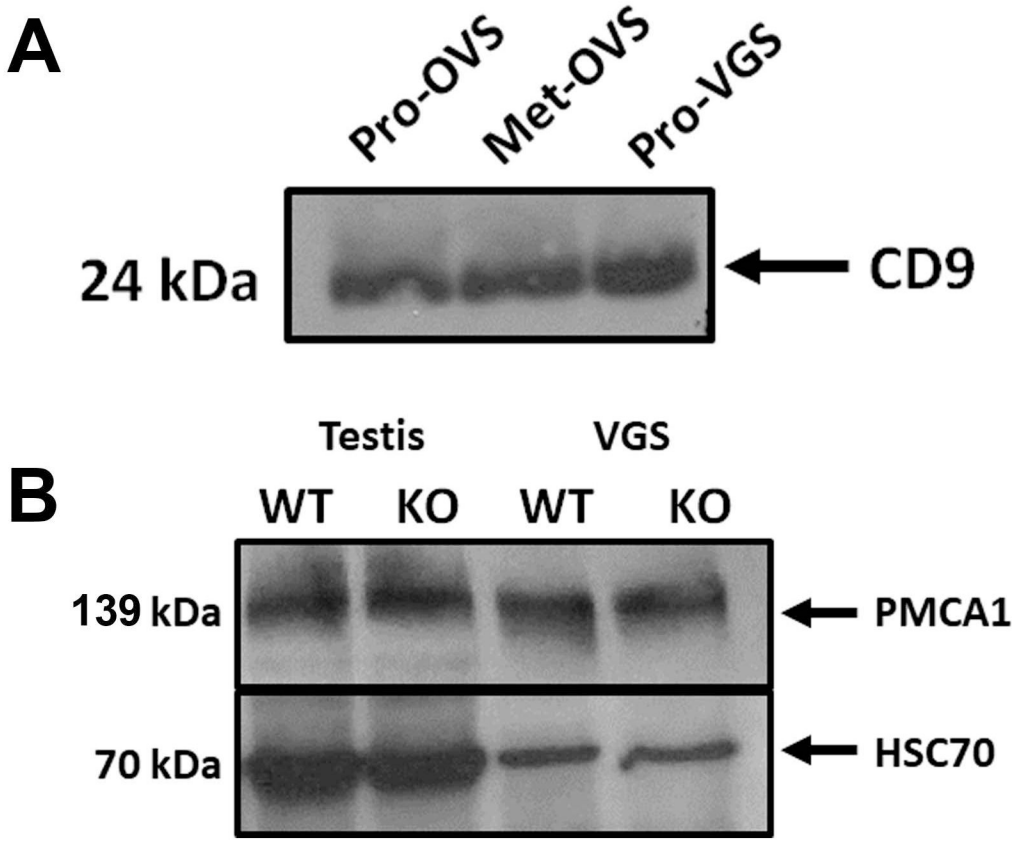

FIGURE 2:

Vaginosomes (VGS) are characterized biochemically as EVs by the presence of CD9 and HSC70, and contain PMCA1 in their cargo. A) Western blot showing the presence of CD9 (24 kDa) on proestrus VGS (Pro-VGS). Positive controls were proestrus and metestrus oviductosomes (Pro-OVS and Met-OVS. **B)** Western blot showing VGS collected from WT and *Pmca4* KO VLF carrying PMCA1 (139 kDa). WT and *Pmca4* KO testis protein lysates were used as positive controls, while HSC70 was used as a loading control and extracellular vesicular marker.

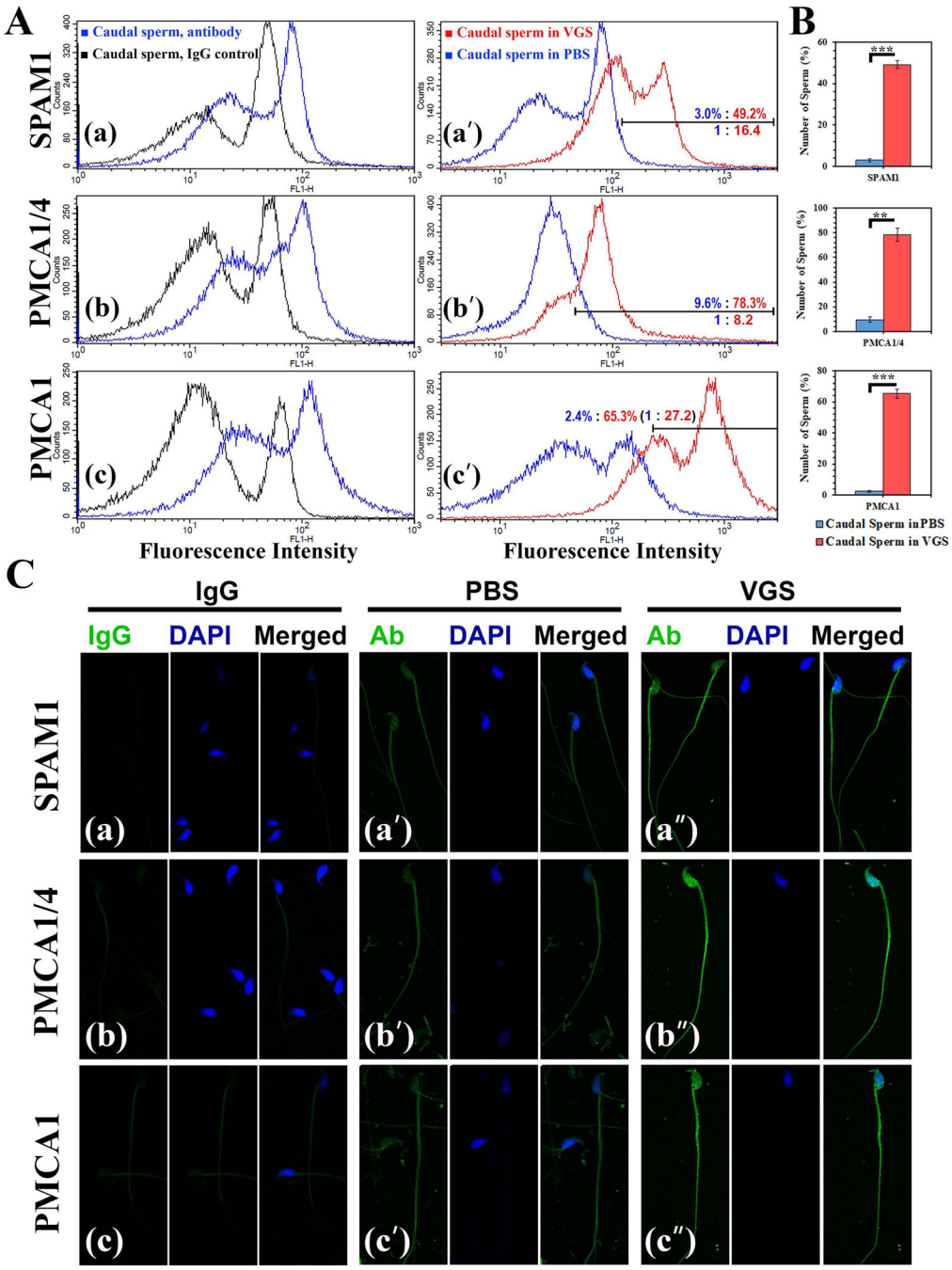

FIGURE 3:

VGS are capable of delivering PMCAs and SPAM1 to caudal sperm following co-incubation. A) Flow cytometry reveals the specificity of the antibodies: **a)** anti-SPAM1, **b)** anti-PMCA1/4, and **c)** anti-PMCA1 show sperm with a right peak shift of fluorescence intensity, compared to the control treated with the IgG (rabbit, PMCA1 and SPAM1; mouse; PMCA1/4). Sperm aliquots in PBS or VGS re-constituted in PBS were incubated for 30 min, and subsequently washed and processed for immunofluorescence. **A-a′, b′, c′**) Fluorescence was quantified in 50,000 cells for each sample, and the region with the highest

intensity marked. The % of cells in this region reveals increases in frequencies with 16.4-fold, 8.2-fold, and 27.2-fold for SPAM1, PMCA1/4, and PMCA1 for sperm in VGS, compared to those in PBS. **B**) When the means of the % of PBS- and VGS-co-incubated cells in the marked region were analyzed by a *t*-test, the differences were significant ($P<0.01$) for each of the proteins (n=3). **C**) Confocal images of sperm immunolabeled for SPAM1, PMCA1/4, and PMCA1 are seen following co-incubation in PBS (**a′, b′, c′**) and VGS (**a′′, b′′, c′′**). IgG control of each antibody is seen in (**a, b, c**). The signals (green) are most intense in **a′′, b′′, and c′′ (**sperm in VGS). The sperm heads are stained blue with DAPI in the middle panel followed by the merged image (Original magnification=×630).

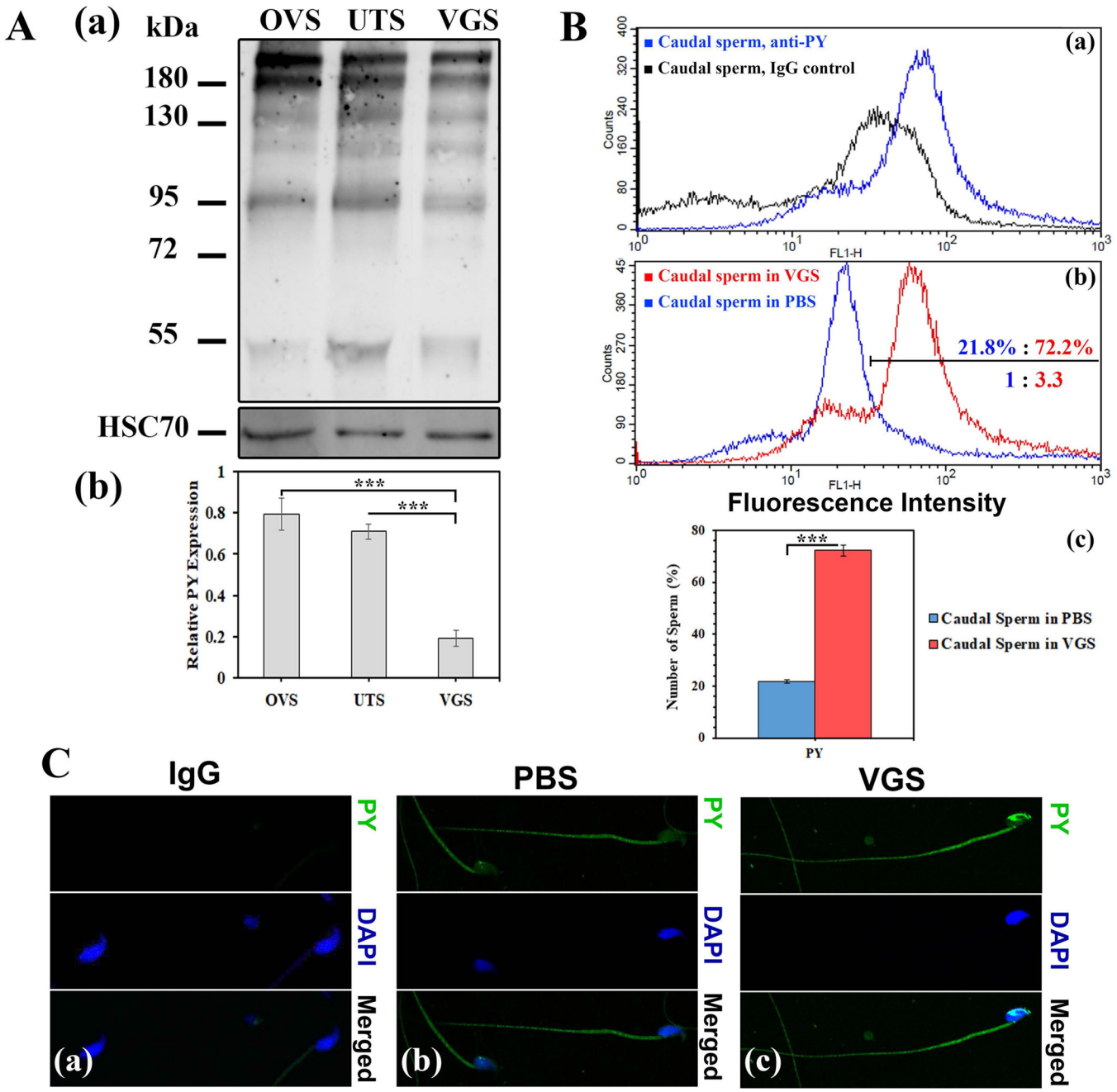

FIGURE 4:

VGS carry tyrosine-phosphorylated proteins which they can deliver to sperm following co-incubation. A-a) Western blot shows 6 tyrosine-phosphorylated proteins (PY) (ranging from MW 55 to >180 kDa) in the cargoes of VGS and uterosomes (UTS), using oviductosomes (OVS) as a positive control. The membrane was stripped and re-probed for HSC70, as a loading control (40 μg protein/lane) to assess the relative intensities of the protein bands. **A-b**) For the 95 kDa band, the intensities for OVS and UTS were significantly ($P<0.001$) higher than that in VGS (n=3). **B-a)** Flow cytometric analysis was performed on 50,000 cells for each sample. The specificity of the anti-phosphotyrosine (PY)

antibodies used is seen by the right peak shift of fluorescence intensity, compared to the IgG control. **B-b)** The graph shows a right peak shift in fluorescence intensity after 30 min co-incubation, with the highest fluorescence intensity (the gated or marked region) displayed by 72.2% of sperm in VGS compared to 21.8% of those in PBS. **B-c)** The difference in the frequencies of the cells in the marked region is significant ($P<0.001$), ($n=3$). **C)** Indirect immunofluorescence shows the localization of PY on the sperm head and flagellum, following co-incubation in PBS and VGS (**C-b and c**), with more intense staining in the latter after PY uptake and none seen in the IgG control (**C-a**). (Original magnification = ×630).

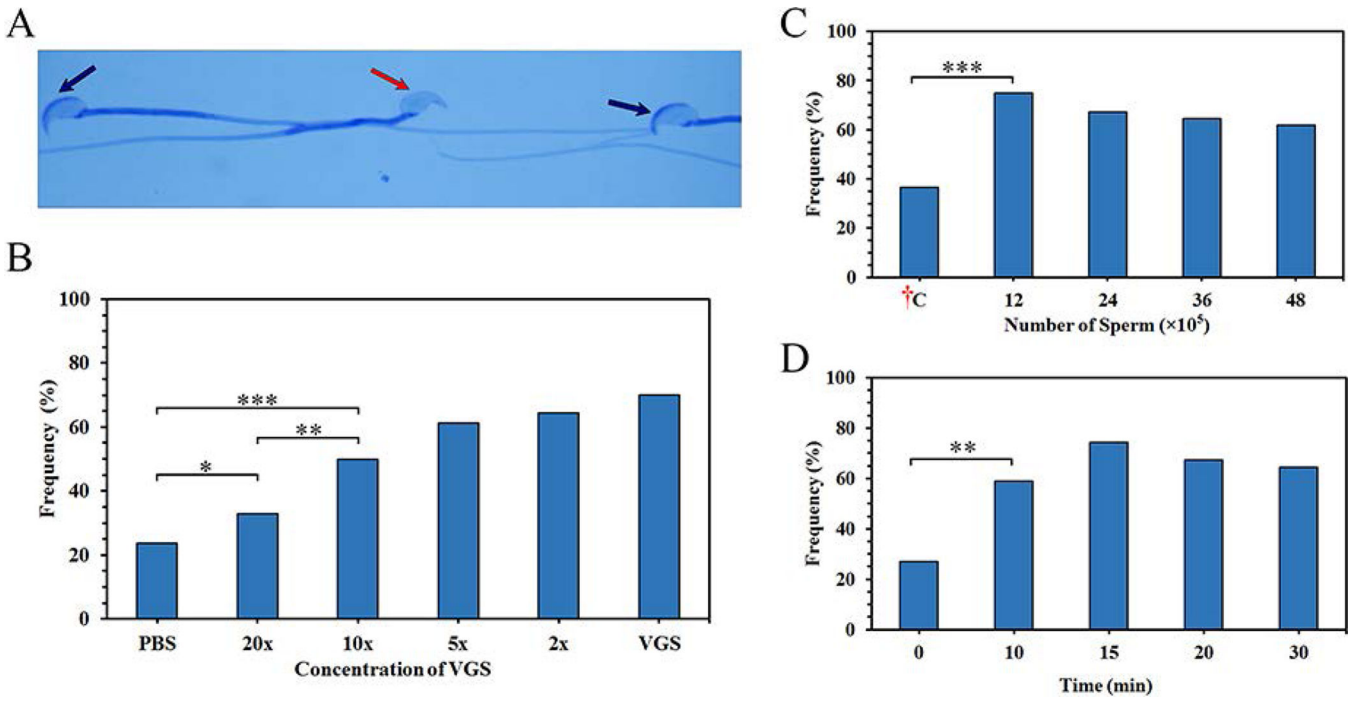

FIGURE 5:

Sperm-VGS interaction *in vitro* and *in vivo* increases the frequency of acrosome-reacted (AR) sperm: *in vitro* response is dose-dependent. A) The acrosomal status of sperm was detected via Coomassie Blue staining after VGS co-incubation. Sperm with an intact acrosomal cap are shown by black arrows, while a missing cap after the acrosome reaction is shown by the red arrow. **B)** Sperm co-incubated in varying concentrations of the VGS (undiluted, 2x, 5x, 10x, 20x diluted VGS) or PBS for 30 min show a dose-response relationship. Using $\chi 2$ analysis, there is a significant (*=P<0.05, **=P<0.01, and ***=P<0.001) increase in AR between samples co-incubated with PBS and 20x / 10x dilution. **C)** Different numbers (12, 24, 36, 48 × 10^5) of sperm were deposited in the vaginas of superovulated mice and the rate of AR compared to the *ex vivo* control: †C (48 × 10^5). Chi-squared ($\chi 2$) analysis shows a significant (P<0.001) increase between the samples and control. **D)** Sperm (36 × 10^5) were deposited in the vaginas for different time periods (0–30 min). The percentages of AR sperm seen after 10 min and beyond were significantly (P<0.01) increased, compared to that of the start point (0 min). Increases between 10 and 30 min were insignificant.

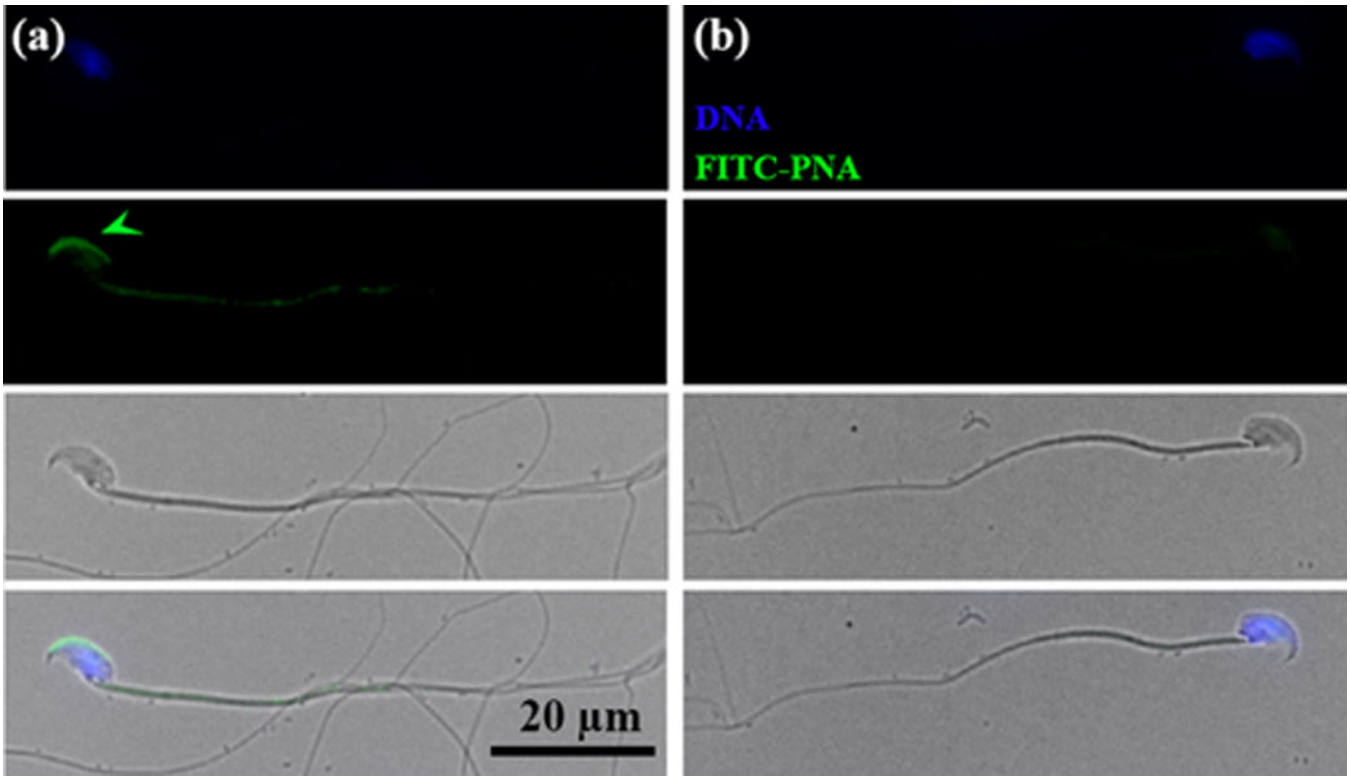

FIGURE 6:

Detection of acrosome-intact (AI) and acrosome –reacted (AR) sperm via FITC-PNA staining of the acrosomal matrix. a) An AI sperm is seen with the green FITC-PNA staining (arrowed) of the acrosomal matrix. **b**) An AR sperm is seen without the acrosomal matrix staining. Phase contrast images are seen below sperm with the acrosomal matrix present/absent, followed by the merged images.

Table 1.

Rates of acrosome-reacted sperm after co-incubation of sperm with PBS (as control) or VGS re-constituted in PBS.

		Number (%)	
Incubation time (min)	**Status**	**Control**	**VGS**
0	**AR**	115 (*32.03*)	107 (*31.02*)[a,d,f]
	No AR	306	316
	Total	421	423
10	**AR**	91 (*25.78*)[b]	405 (*83.97*)[a,b]
	No AR	328	88
	Total	419	493
20	**AR**	104 (*30.98*)[c]	429 (*92.37*)[c,d]
	No AR	324	49
	Total	428	478
30	**AR**	123 (*28.12*)[e]	403 (*95.36*)[e,f]
	No AR	348	20
	Total	471	423
Grand Total	**AR**	433 (29.23)[g]	1344 (75.68)[g]
	No AR	1306	473
	Total	1739	1817

AR: Acrosome reaction. Identical letters refer to significant differences.

[a] P<0.001: between before and after 10 min co-incubated with VGS;

[b] P<0.001: between co-incubation with PBS as a control and VGS for 10 min;

[c] P<0.001: between co-incubation with PBS as a control and VGS for 20 min;

[d] P<0.001: between before and after 20 min co-incubated with VGS;

[e] P<0.001: between co-incubation with PBS as a control and VGS for 30 min;

[f] P<0.001: between before and after 30 min co-incubated with VGS;

[g] P<0.001: between the grand control and co-incubated with VGS.